7
Temperature Dependent Transport Studies at 2D/3D Heterointerfaces

7.1 INTRODUCTION

In the earlier chapters, we have studied the photo and gas sensing behavior of MoS_2/Si and MoS_2/GaN heterostructures. However, the charge transport mechanism and the device physics under thermal excitation is not studied yet. Therefore, in this chapter, we studied the effect of temperature on various parameters such as barrier height, ideality factor, and current density at the 2D/3D heterointerfaces.

The I-V characteristics of MoS_2/Si and MoS_2/GaN heterojunctions exhibit a rectifying behavior at room temperature. For in-depth qualitative analysis of the rectifying behavior, we have performed the temperature-dependent I-V measurement of MoS_2/Si and MoS_2/GaN heterojunctions ranging from 100 to 500 K. Our results reveal that temperature vigorously affects the barrier height and ideality factor of both the devices. The barrier height can easily be tuned by changing the junction temperature. The increase in temperature results in increasing the thermally induced charge carriers across the interface, which leads to raising the on-current.

7.2 TEMPERATURE DEPENDANT BEHAVIOR OF MOS_2/Si HETEROJUNCTION

7.2.1 Fabrication and characterization of MoS_2/Si heterojunction

The detailed fabrication and characterization procedure of MoS_2/Si heterojunction have already been discussed in chapter 4. In summary, we have fabricated MoS_2/Si heterojunction using mechanical exfoliation process. Au and Al contacts are made on MoS_2 and silicon, respectively, using the thermal evaporator technique. The spectroscopic and microscopic characterization was done through Renishaw Raman spectrometer and Park Systems atomic force microscopy.

7.2.2 Tunable rectifier behavior at MoS_2/Si heterojunction

To investigate the temperature dependence of MoS_2/Si heterointerface, we have fabricated MoS_2/Si heterojunction by exfoliating MoS_2 on top of the silicon substrate. The 3D schematic illustration of the device is shown in Figure 7.1. Al makes the ohmic contacts with p- and n-type silicon, as shown in Figure 7.2(a). For making ohmic contact with p-Si, it is to be annealed for 15 mins at 300˚C in N_2 ambiance. The exfoliated flake of MoS2 makes an ohmic contact with Au, as shown in Figure 7.2(b).

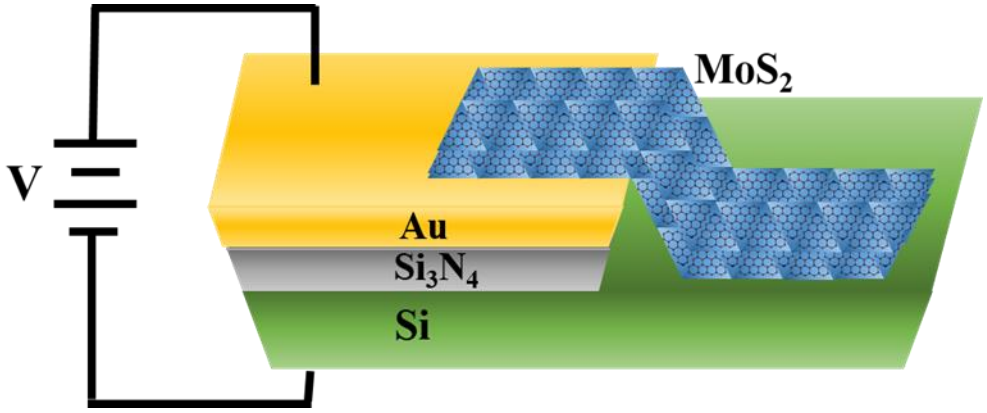

Figure 7.1: Three-dimensional schematic diagram of the device.

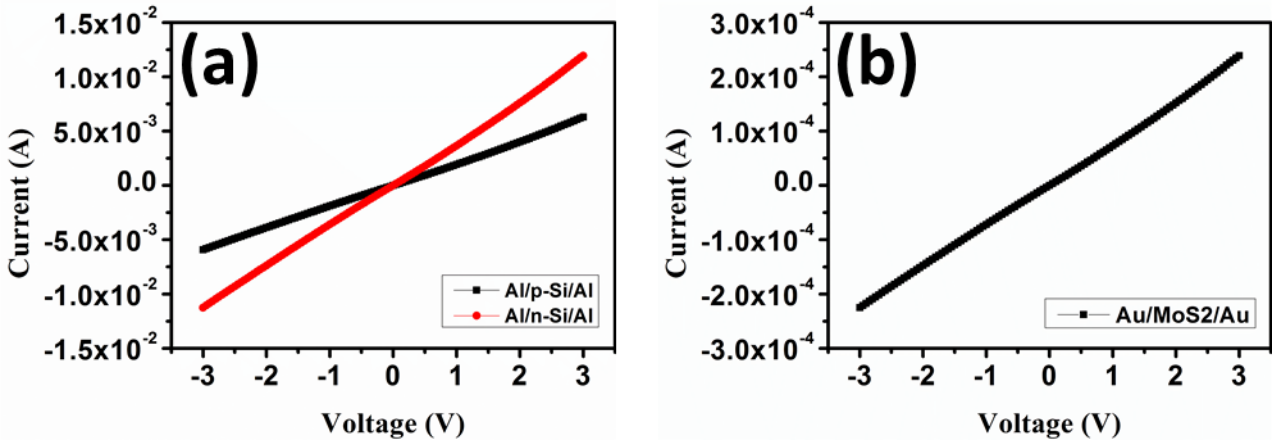

Figure 7.2: Current–voltage characteristics for (a) Al/p-Si/Al and Al/n-Si/Al configuration and (b) Au/MoS_2/Au configuration.

Figure 7.3(a) shows the I-V characteristics of MoS_2/p-Si heterojunction measured at different temperatures from 100 to 500 K. The MoS_2/p-Si interface exhibits rectifying behavior. As we increased the temperature of the device from 100 K to 500 K, the current enhance due to the increment of carriers' density at the interface. This increment in carrier density at the interface of heterostructure attributed to thermally generated charge carriers. The current at a temperature of 500 K is approximately five times higher than that of 100 K in the MoS_2/p-Si device at 3V, as shown in Figure 7.3(a). Moreover, we have also deposited FL-MoS_2 on n-type Si. And the I-V characteristics of MoS_2/n-Si heterostructure are investigated at different temperatures (T: 100, 200, 300, 400, and 500 K), as depicted in Figure 7.3(b), which clearly demonstrates that a barrier is formed at the MoS_2-silicon interface. In the MoS_2/n-Si device, it was found that the current enhances approximately two times over a temperature change of 100 K to 500 K at 3V.

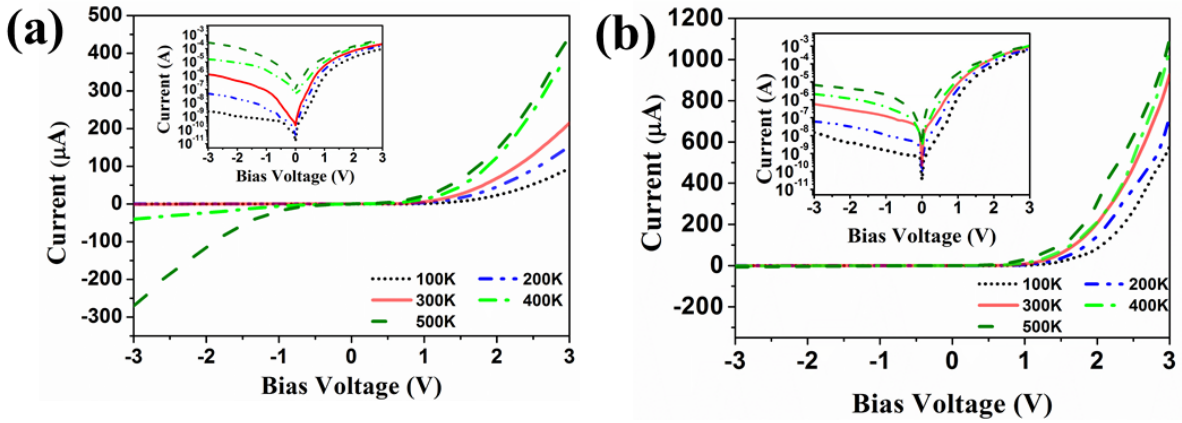

Figure 7.3: Current-voltage characteristics measured at different temperatures (100, 200, 300, 400 and 500 K) for (a) MoS_2/p-Si device (b) MoS_2/n-Si device. The inset shows current on a log scale.

The current flowing across the MoS_2/n-Si heterojunction forming an energy barrier at the interface that can be approximated by the following standard thermionic emission equation(Crowell and Sze, 1966).

$$I = I_0\left[exp\left(\frac{qV}{\eta k_B T}\right) - 1\right] \tag{7.1}$$

where I_0 is given as:

$$I_0 = SA^*T^2 exp\left(-\frac{q\Phi_B}{k_B T}\right) \tag{7.2}$$

where I_0 is the reverse saturation current, q is the electronic charge, η is the ideality factor, k_B is the Boltzmann's constant, T is the operating temperature, S is the active contact area, A^* is the effective Richardson's constant (112 A cm^{-2} K^{-2} for n-Si)(Tung et al., 1986), and φ_B is the Schottky barrier height. From Eq. (7.2) the Schottky barrier height φ_B can be expressed as:

$$\varphi_B = \frac{k_B T}{q}\, ln\left(\frac{SA^*T^2}{I_0}\right) \tag{7.3}$$

The fitting of experimental data shown in Figure 7.3(b) to above equations gives the values of the ideality factor at different temperatures. The ideality factor registered a decrement with an increase in temperature. For the MoS_2/n-Si device, the barrier height is calculated by using Eq. (7.3), ranges from 0.185 to 0.780 eV with an increase in temperature (100-500 K). Table 7.1 summarizes the various parameters calculated for p- and n-Si devices, including barrier height, ideality factor, and current density. Table 7.1 shows that the barrier height for the n-Si device increases with increasing temperature, which is in contrast to Figure 7.3(b). In accordance with Figure 7.3(b), current increases with an increase in temperature. These contradictory results indicate that the thermally induced electrons govern the flow of current across the heterojunction, and the barrier height does not play an active role in current conduction.

Table 7.1: Summary of data taken at different temperatures at MoS_2-silicon heterojunction.

Temperature (K)	Φ_B (eV)	ideality factor	J (A/m²)	
	n-Si		p-Si	n-Si
100	0.185	7.3	2.04×10^6	1.39×10^6
200	0.361	4.8	3.25×10^6	2.26×10^6
300	0.522	4.6	4.56×10^6	2.89×10^6
400	0.677	3.8	8.58×10^6	4.09×10^6
500	0.780	2.9	9.63×10^6	4.28×10^6

7.3 TEMPERATURE DEPENDANT BEHAVIOR OF MOS_2/GAN HETEROJUNCTION

7.3.1 Fabrication and characterization of MoS_2/GaN heterojunction

The 1×1 cm^2 GaN/Al2O3 sample was loaded into the sputtering chamber, and the chamber was maintained at a base pressure of 2×10^{-6} mbar for deposition of 300 nm of Si3N4. The deposition was done using a mixture of Ar (45 sccm) and N2 (10 sccm) with a DC power of 90 W at room temperature. For the growth of Mo film, the Mo target (99.99% purity) was sputtered at a temperature of 600 ˚C for 20 min. During sputtering, the chamber pressure and DC power were controlled to be 6.5×10^{-3} mbar and 40 W, respectively. The Mo deposited film was then sulfurized in the sulfur-rich environment at 600 ˚C in the presence of Ar for 30 min. A 150/10 nm Au/cr and a 150 nm Al was deposited on top of MoS_2 and GaN film, respectively, using a thermal evaporator.

Optical microscopy (Touptek photonics), Nova Nano FE-SEM 450 (FEI), Renishaw Raman spectroscopy (514 nm laser excitation wavelength), Multimode Scanning Probe Microscope (Bruker), X-ray photoelectron spectroscopy (Scienta Omicron, Germany, using monochromatized Al Kα (1486.7 eV) radiation source), and Parametric Analyzer (Keithley 4200-SCS) were employed to characterize the fabricated device.

7.3.2 Tunable rectifier behavior at MoS_2/GaN heterojunction

We grew a multilayer MoS_2 film by sputtering molybdenum on top of the GaN substrate, followed by the sulfurization process, as shown in chapter 4. The details of the deposition method are given in the experimental section. The surface morphology of the deposited MoS_2 film on the GaN substrate was characterized by FE-SEM technique. Figure 7.4(a) shows the FE-SEM image at the interface of MoS_2 and GaN and Figure 7.4(b-d) displays the FE-SEM images of the center part of deposited MoS_2 film with different magnifications, confirming the continuity and homogeneity of the deposited film.

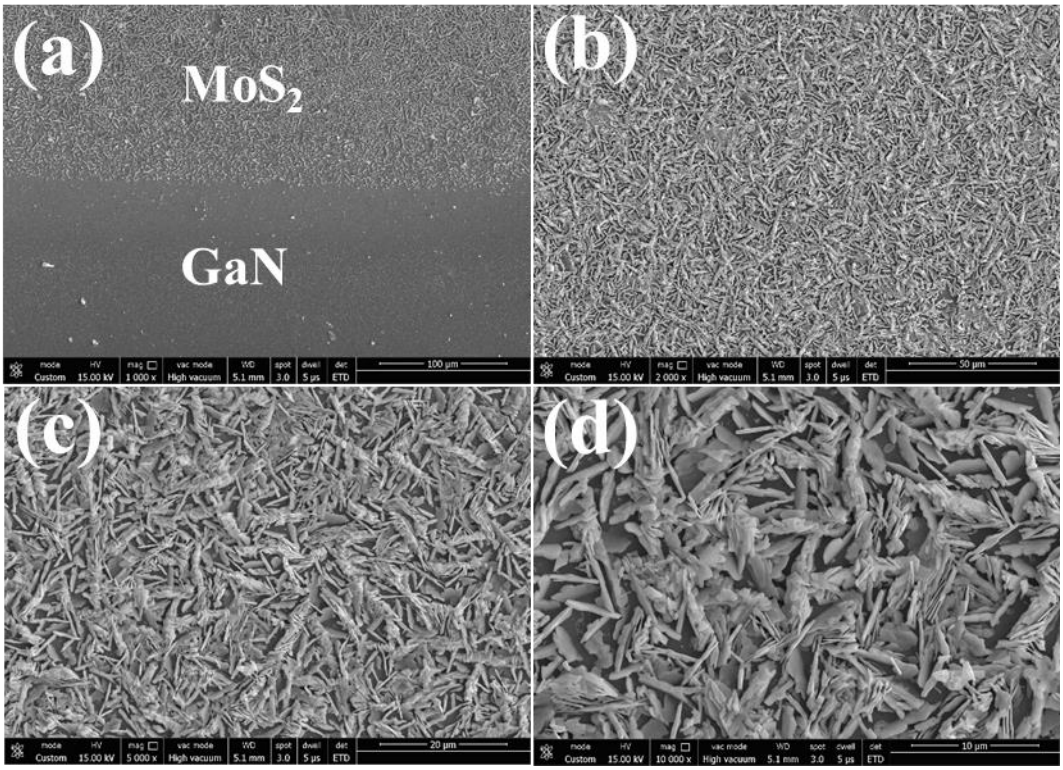

Figure 7.4: FE-SEM images of MoS_2 deposited on GaN film (a) at the edges and (b,c,d) at the central zone with different magnifications.

A schematic illustration and the optical image of a fabricated MoS_2/GaN heterojunction is shown in Figure 7.5(a) and 7.5(b), respectively. In the Raman spectra (Figure 7.5(c)), two different peaks were obtained at 382 and 407 $cm^{-1,}$ which corresponds to in-plane (E^1_{2g}) and out-of-plane (A_{1g}) vibrational modes of the deposited MoS_2 film, respectively. The difference between the two vibrational modes ~25 cm^{-1}, indicates a multi-layer MoS_2 film. A continuous and uniform surface morphology of the grown MoS_2 film was also observed by 2D and 3D (inset) AFM images, as shown in Figure 7.5(d).

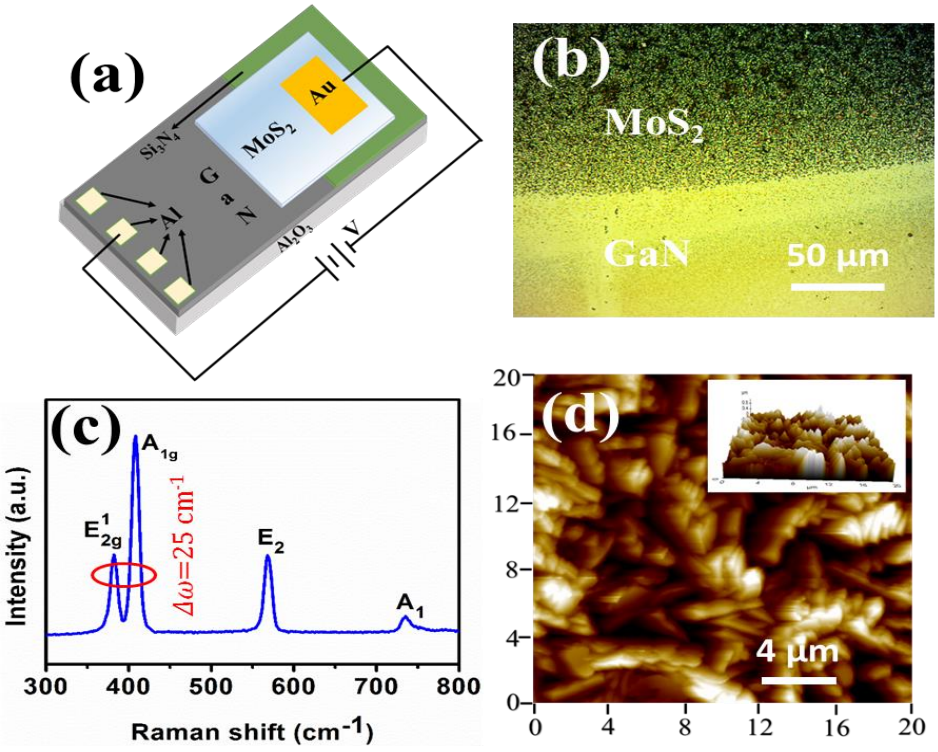

Figure 7.5: (a) Schematic diagram of the fabricated device (b,c) Optical image and Raman spectra of MoS_2/GaN heterojunction (d) Tapping-mode AFM image of MoS_2 film grown on GaN substrate. Inset shows the 3D image of a grown MoS_2 film.

To study the behavior of the fabricated device, electrical characterization was done at room temperature, as displayed in Figure 7.6. The Au and Al make ohmic contact with MoS_2 and GaN, respectively, while MoS_2-GaN interface exhibits a rectifying behavior. Figure 7.7(a) shows the I-V characteristics of the device measured at different operating temperatures (100-500 K). All the measured I-V characteristics exhibit a rectifying behavior. However, the rectifying behavior dampened with an increase in operating temperature. This dampening behavior is due to thermally induced electrons at a higher value of temperatures, which increases the carrier density at the MoS_2/GaN heterojunction. With an increase in temperature, the I-V characteristics move closer to ohmic behavior.

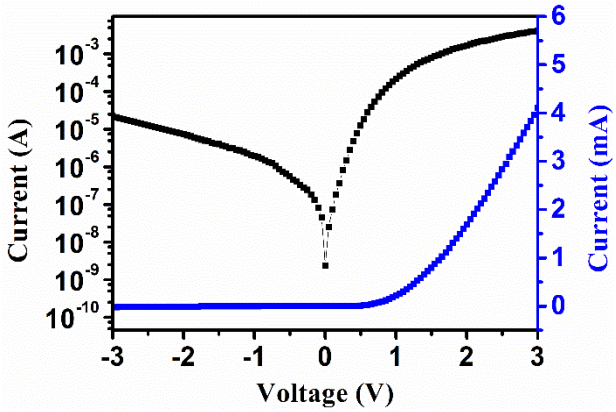

Figure 7.6: (a) Current-voltage characteristics of MoS_2/GaN heterojunction using log and linear scale at room temperature (b) Energy band diagram of MoS_2/GaN heterojunction.

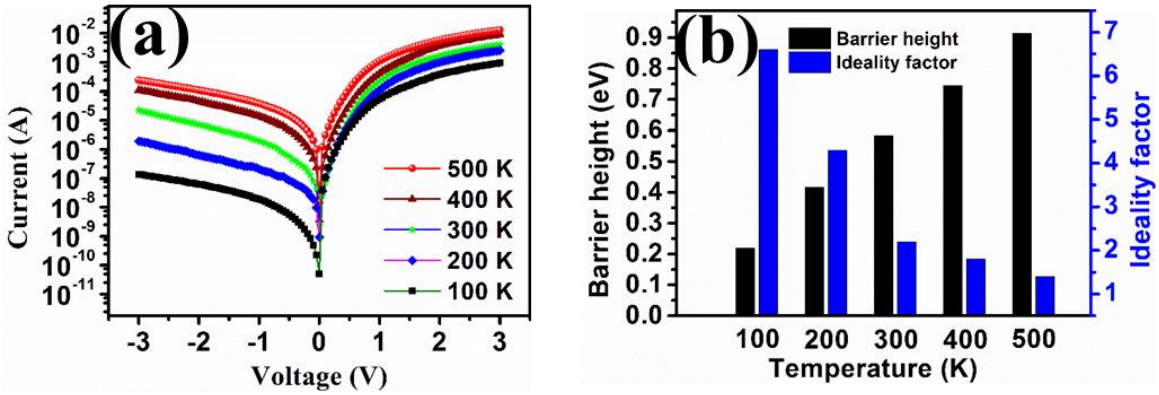

Figure 7.7: (a) Current-voltage characteristics of MoS_2/GaN heterojunction using log scale at different temperatures. (b) The bar graph depicting the variation in barrier height and ideality factor with temperature.

The barrier height and ideality factor at MoS_2/GaN heterointerface were calculated using the standard thermionic emission as already given in Eq. (7.1) to (7.3). A barrier height of 0.219 eV and ideality factor having a value of 6.6 was measured at 100 K, as shown in Figure 7.7(b). The barrier height increases with increase in temperature, and it reaches to a value of 0.915 eV at 500 K. While the ideality factor decreases with increase in temperature and it reaches to a value of 1.4 at 500 K. A similar kind of observation has also been seen in the MoS_2/Si heterojunction based devices. With an increase in temperature, both current and barrier height across the MoS_2/GaN heterointerface increase because the thermally induced electrons play the dominant role in the current conduction process.

7.4 CHAPTER SUMMARY

In conclusion, we studied the charge transport mechanism of the MoS_2/Si and MoS_2/GaN heterointerfaces under thermal excitation. We observe that barrier height and current density in both the devices increases with an increase in temperature. While the ideality factor decreases with an increase in temperature. At low temperature, the charge carriers could not cross the energy barriers at the interface due to their low energy. With the increase in temperature, the energy of the charge carriers also increases, enabling them to cross the energy barrier, and hence current density increases.